Supporting Information

Anions Influence the Relaxation Dynamics of Mono-μ_3-OH Capped Triangular Dysprosium Aggregates

Li Zhang,[†,‡] *Peng Zhang,*[†,‡] *Lang Zhao,*[†] *Jianfeng Wu,*[†,‡] *Mei Guo,*[†,‡] *Jinkui Tang**[†]

[†]State Key Laboratory of Rare Earth Resource Utilization, Changchun Institute of Applied Chemistry, Chinese Academy of Sciences, Changchun 130022, P. R. China
[‡]University of Chinese Academy of Sciences, Beijing, 100049, P. R. China

Corresponding Author
*E-mail: tang@ciac.ac.cn.

Table of contents

Figure S1. IR spectra of complexes **1**-**4** S1
Figure S2. Coordination polyhedra of Dy^{III} ions observed in **1**-**4**....S1
Figure S3. Packing arrangement for complexes **1** and **2**....S2
Figure S4. Packing arrangement for complexes **3** and **4**....S3
Figure S5. Field dependences of magnetization for **1**-**4**....S4
Figure S6. Temperature dependence of the in-phase and out-of-phase ac susceptibility under 0 Oe and 300 Oe dc field for **1**....S4
Figure S7. The Cole-Cole diagrams for **1** at different temperatures under a zero dc field....S5
Figure S8. Out-of-phase ac susceptibility (χ'') collected on **1** at 1.9 K under the indicated dc field S5
Figure S9. The Cole-Cole diagrams for **1** at different temperatures under a 300 Oe dc field....S5
Figure S10. Temperature dependence of the in-phase and out-of-phase ac susceptibility under 0 Oe and 1000 Oe dc field for **2**....S6
Figure S11. The Cole-Cole diagrams for **2** at different temperatures under a 1000 Oe dc field....S6
Figure S12. Plots of natural logarithm of χ''/χ' vs. $1/T$ for **3** and **4** under a zero dc field....S6
Figure S13. Dependence of the out-of-phase signal of **3** on applied dc field strength at 1.9 K, 997 Hz....S7
Figure S14. Dependence of the out-of-phase signal of **4** on applied dc field strength at 1.9 K, 997 Hz....S7
Figure S15. Magnetization relaxation time, $\ln\tau$ versus T^{-1} for **4** under a 900 Oe dc field....S7
Scheme S1. Binding mode of the ligand HL^{2-} in complexes **1**-**4**....S8
Table S1. Structural parameters [Å, °] for central $[Dy_3O_4]$ core for complexes **1**-**4**....S9

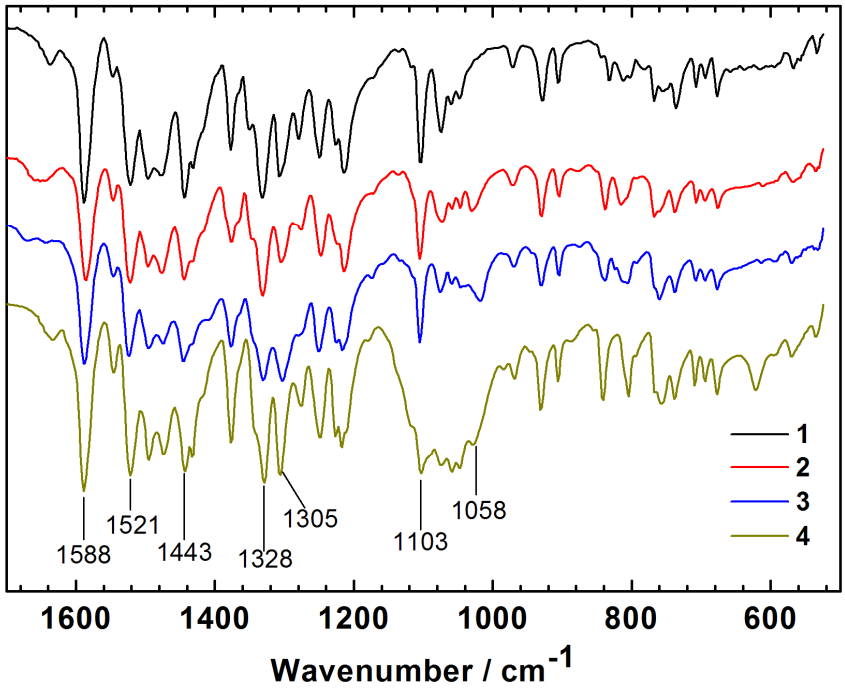

Figure S1. IR spectra of complexes **1**-**4**.

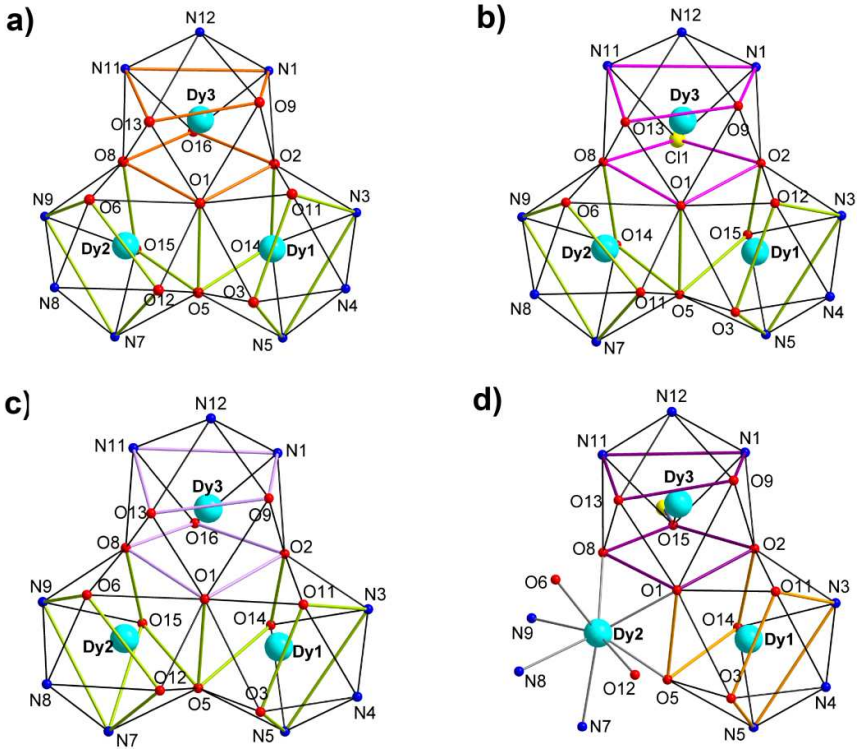

Figure S2. a)-d) Coordination polyhedra of Dy^{III} ions observed in **1**-**4**.

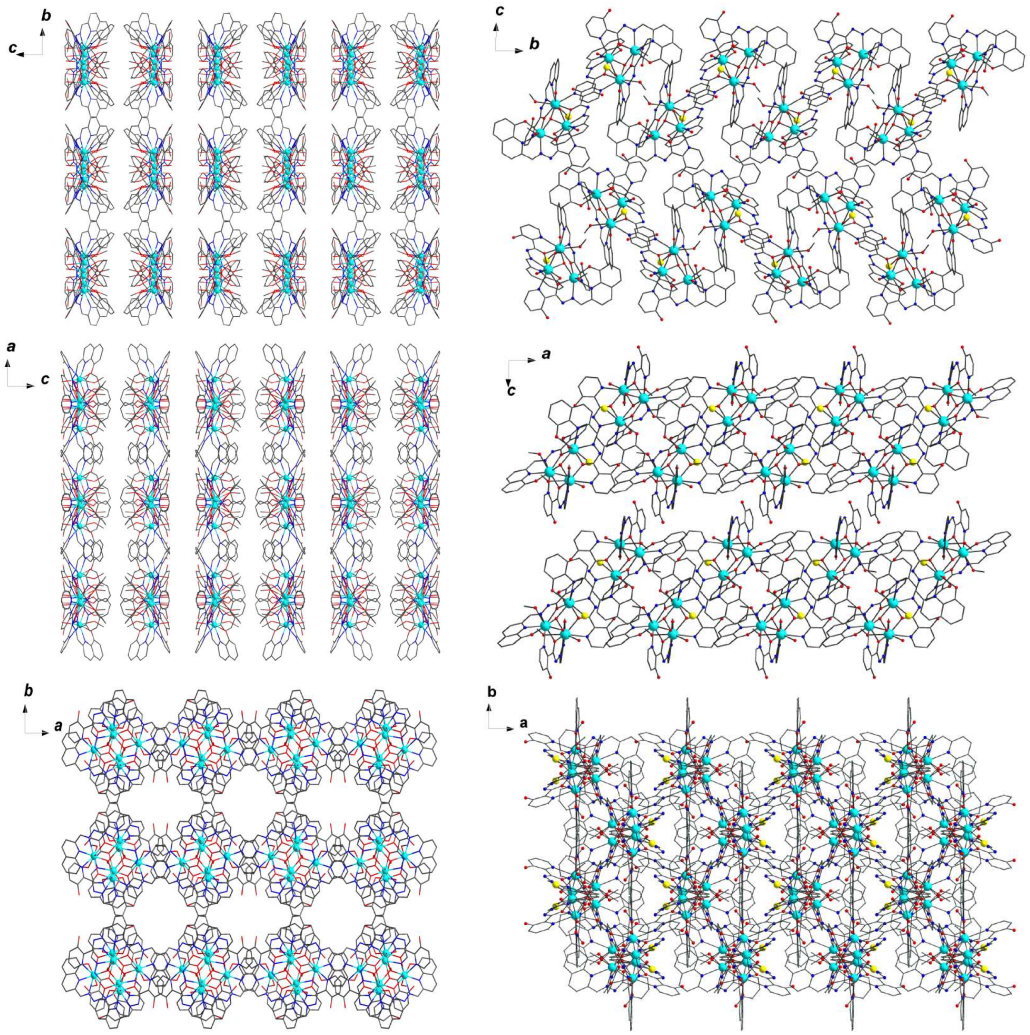

Figure S3. Packing arrangement along the crystallographic a, b, and c-axis for complex **1** (left) and **2** (right). Color code: turquiose, Dy; red, O; blue, N; yellow, Cl.

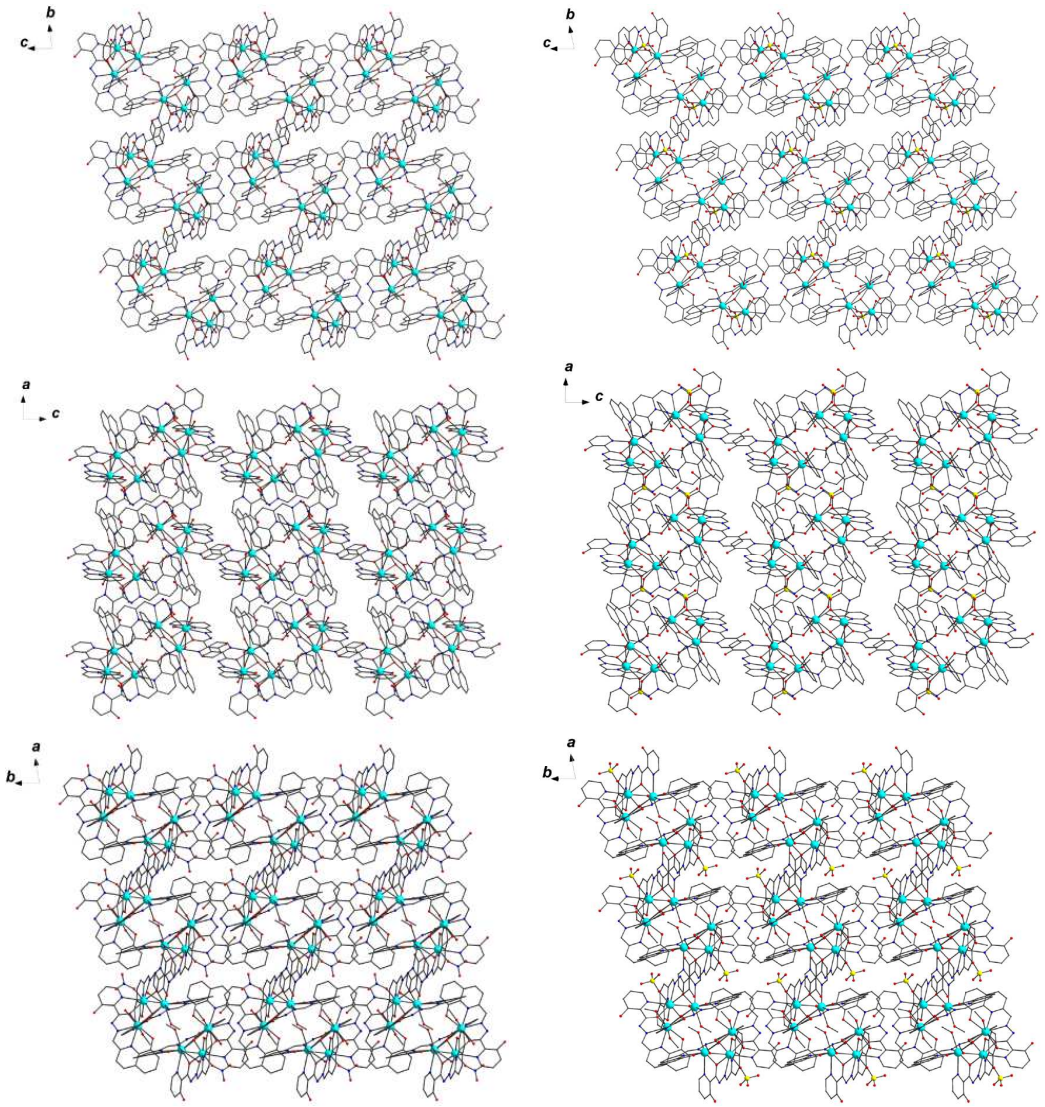

Figure S4. Packing arrangement along the crystallographic a, b, and c-axis for complex **3** (left) and **4** (right). Color code: turquiose, Dy; red, O; blue, N; yellow, Cl.

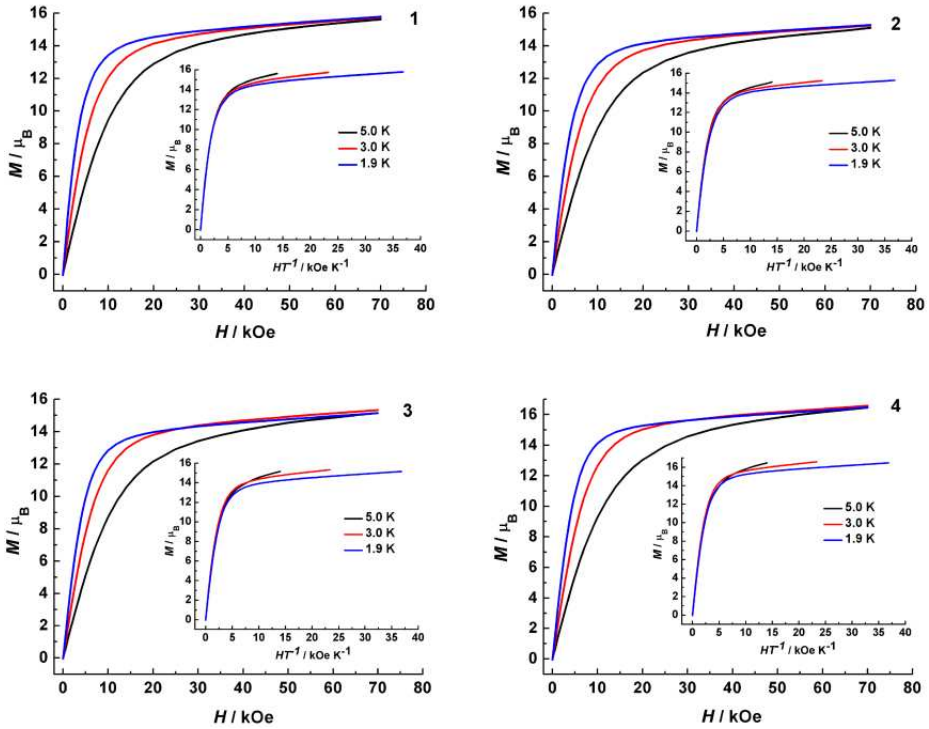

Figure S5. Field dependences of magnetization in the field range 0-70 kOe and at the range of 1.9-5.0 K. Insets: Plots of the reduced magnetization *M* versus *H*/*T* for **1**-**4**.

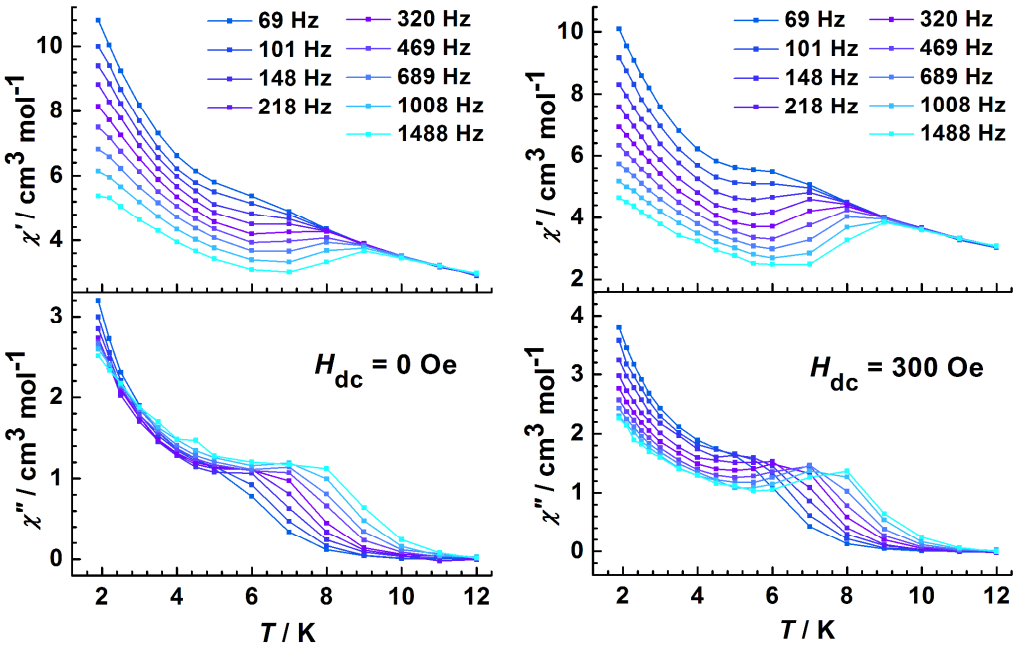

Figure S6. Temperature dependence of the in-phase (top) and out-of-phase (bottom) ac susceptibility under 0 Oe (left) and 300 Oe (right) dc field for **1**.

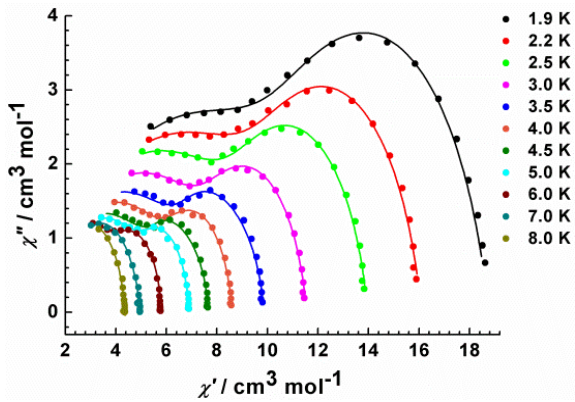

Figure S7. The Cole-Cole diagrams for **1** at different temperatures under a zero dc field. The solid lines represent the fit using the sum of two modified Debye functions.

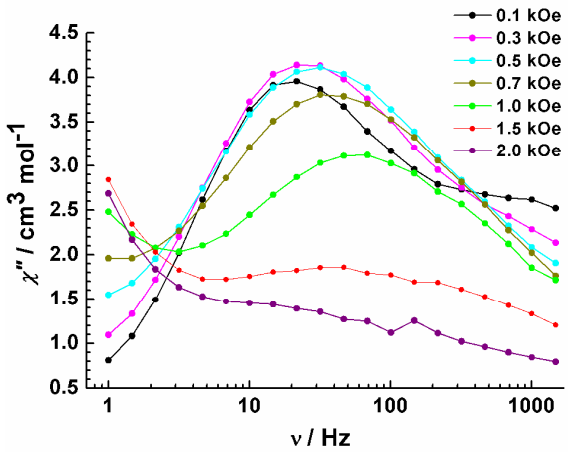

Figure S8. Out-of-phase ac susceptibility (χ'') collected on **1** at 1.9 K under the indicated dc field.

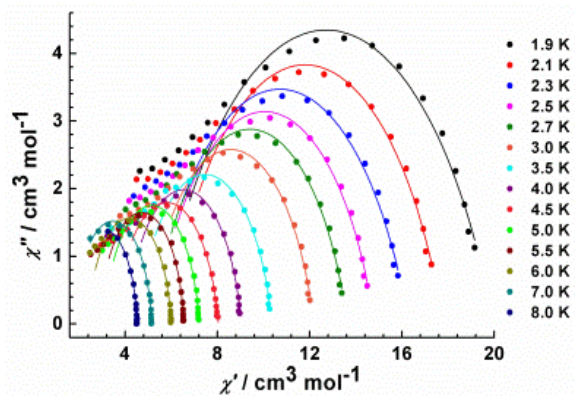

Figure S9. The Cole-Cole diagrams for **1** at different temperatures under a 300 Oe dc field. The solid lines represent the fit obtained with a generalized Debye model.

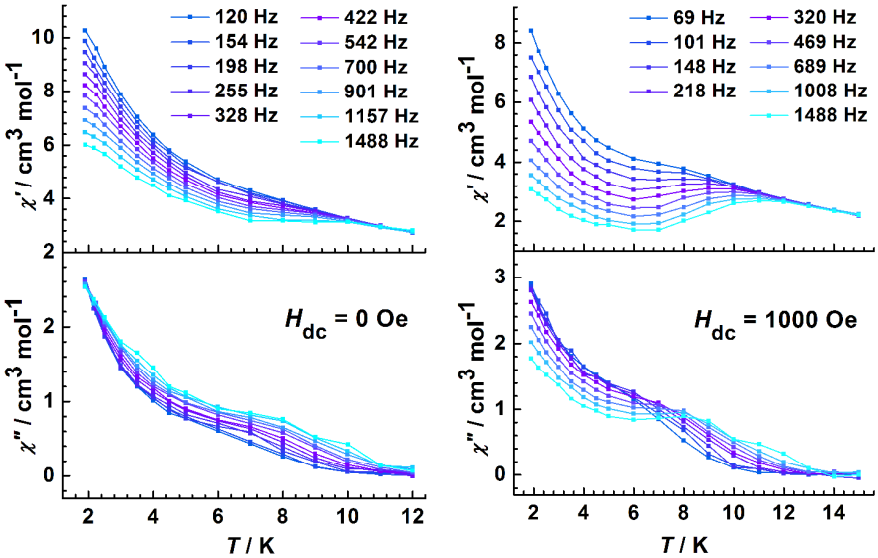

Figure S10. Temperature dependence of the in-phase (top) and out-of-phase (bottom) ac susceptibility under 0 Oe (left) and 1000 Oe (right) dc field for **2**.

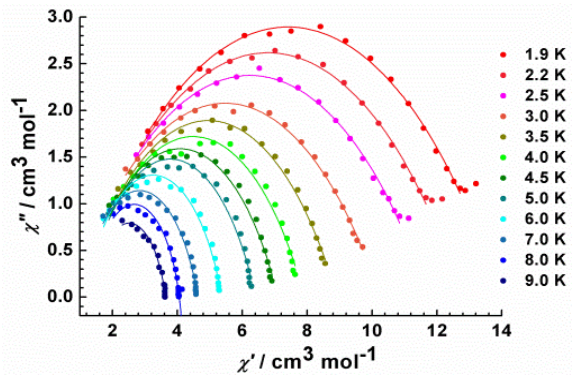

Figure S11. The Cole-Cole diagrams for **2** at different temperatures under a 1000 Oe dc field. The solid lines represent the best fit obtained with a generalized Debye model.

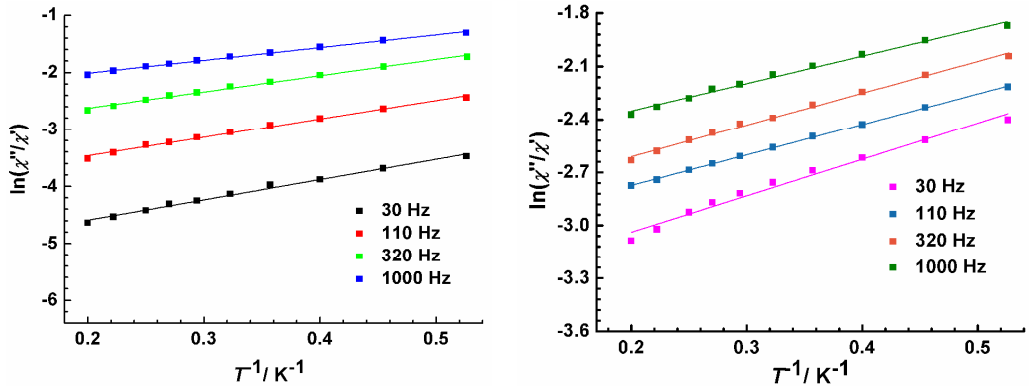

Figure S12. Plots of natural logarithm of χ''/χ' vs. $1/T$ for **3** (left) and **4** (right) under a zero dc field. The solid line represents a fit of the results over the range of 30-1000 Hz.

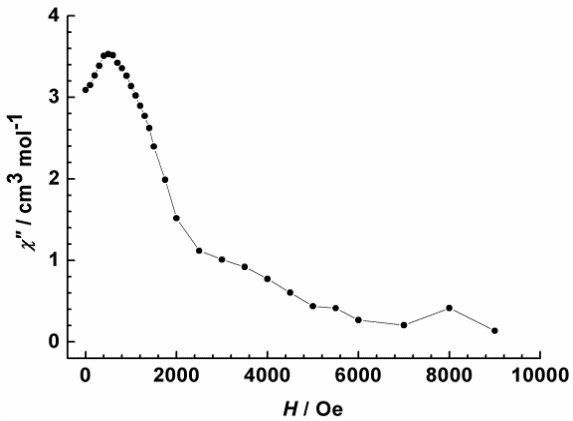

Figure S13. Dependence of the out-of-phase signal of **3** on applied dc field strength at 1.9 K, 997 Hz.

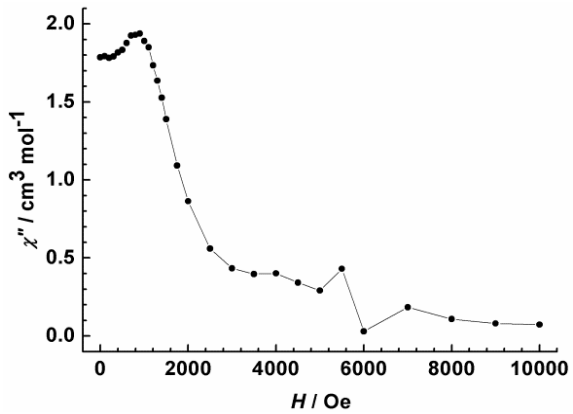

Figure S14. Dependence of the out-of-phase signal of **4** on applied dc field strength at 1.9 K, 997 Hz.

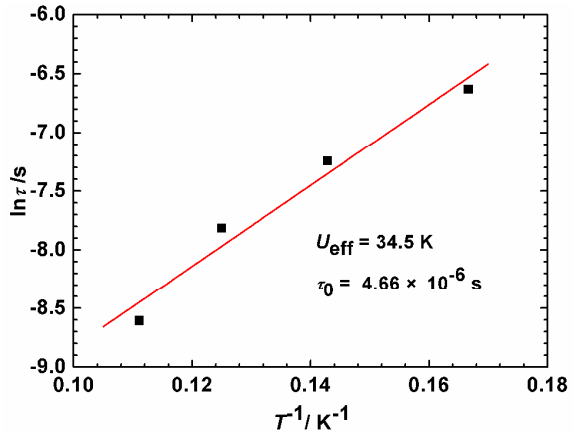

Figure S15. Magnetization relaxation time, lnτ versus T^{-1} for **4** under a 900 Oe dc field. The solid lines correspond to the best fit of the experimental data to the Arrhenius law.

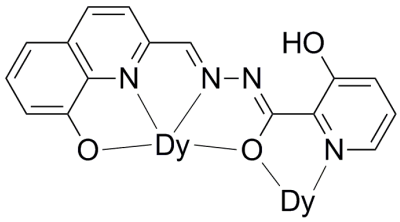

$2.1_12_{12}01_11_101_2$ (μ_2-η^1:η^2:η^1:η^1:η^1)

Scheme S1. Binding mode of the ligand HL^{2-} in complexes **1**-**4**.

Table S1. Structural parameters [Å, °] for central [Dy_3O_4] core for complexes **1**-**4**.

	1	**2**	**3**	**4**
Dy1-O1	2.374(9)	2.400(3)	2.395(5)	2.394(5)
Dy2-O1	2.373(10)	2.365(3)	2.355(5)	2.347(4)
Dy3-O1	2.387(10)	2.367(3)	2.374(5)	2.393(5)
Dy1-O2	2.394(9)	2.398(4)	2.397(5)	2.391(4)
Dy1-O5	2.382(9)	2.369(3)	2.368(6)	2.397(5)
Dy2-O5	2.392(9)	2.412(3)	2.386(6)	2.349(5)
Dy2-O8	2.374(9)	2.381(3)	2.354(5)	2.332(5)
Dy3-O8	2.415(10)	2.412(3)	2.392(6)	2.393(5)
Dy3-O2	2.401(10)	2.394(4)	2.364(5)	2.344(5)
Dy1…Dy2	3.9461(10)	3.9680(4)	3.9366(6)	3.9186(5)
Dy2…Dy3	3.9428(11)	3.9574(4)	3.9310(6)	3.9514(5)
Dy3…Dy1	3.9773(10)	3.9583(4)	3.9614(5)	3.9303(5)
Dy1-O1-Dy2	112.5(4)	112.76(13)	111.9(2)	111.51(19)
Dy2-O1-Dy3	111.9(4)	113.50(13)	112.5(2)	112.93(18)
Dy3-O1-Dy1	113.3(4)	112.26(13)	112.3(2)	110.38(18)
Dy1-O5-Dy2	111.5(4)	112.20(13)	111.8(2)	111.3(2)
Dy2-O8-Dy3	110.8(3)	111.30(13)	111.9(2)	113.5(2)
Dy3-O2-Dy1	112.1(4)	111.40(13)	112.6(2)	112.19(17)
Dy1-Dy3-Dy2	59.766(18)	60.170(7)	59.837(10)	59.625(8)
Dy2-Dy1-Dy3	59.682(19)	59.903(6)	59.699(10)	60.455(8)
Dy3-Dy2-Dy1	60.552(17)	59.927(6)	60.464(10)	59.920(8)
Dy3-$L_{terminal}$	**2.386(10)**	**2.781(14)**	**2.470(7)**	**2.619(6)**
	(Dy3-O_{water})	(Dy3-Cl)	(Dy3-$O_{nitrate}$)	(Dy3-$O_{perchloate}$)